# POSSIBILITY OF DOUBLE CIRCULATION FREQUENCY OPERATION OF STRIPLINE Y-JUNCTION CIRCULATOR

TSUKASA NAGAO
Department of Electrical Engineering, Defense Academy
Hashirimizu, Yokosuka 239 Japan

ABSTRACT

The application of double circulation frequency operation (DCFO) is proposed to a wide band operation of a stripline Y-junction circulator. The DCFO mechanism, bandwidth and experiments are also reported.

## I. Introduction

Any conventional stripline Y-junction circulators are adjusted to operate at a single resonant frequency of circulation. The procedure of their design and operation owes basically to the works of Bosma[1] and Fay and Comstock[2]. Despite the fact that octave bandwidth circulators are available, impedance matching needs some sophisticated impedance transformers over a wide band[3-5]. Bosma reported that theoretical estimation of a bandwidth appeared to be not more than 5 o/o for a crude disk circulator. The author has learned that theoretical results of bandwidth for several composite circulators have not yet exceeded that value. Recently, Wu and Rosenbaum[6] reported that selection of the width of the coupling transmission line significantly improves a wide band operation. However, one may say that all of the works in circulator seem to fall within the category of single circulation frequency operation (SCFO). SCFO is literally based on the way how a circulator is designed under the circulation conditions at a given single frequency of circulation.

If circulator parameters can be fixed from the conditions which are dependent on two different circulation frequencies, the choice of the two different circulation frequencies will determine a bandwidth of DCFO. A DCFO does, as a matter of course, depend on its circulation adjustment.

In this paper, comparison of SCFO and DCFO, the mechanism of DCFO, bandwidth and experiments are reported. Throughout the experiments, any impedance matching transformers external to the stripline Y-junction are excluded.

## II. Circulation conditions of simple ring ferrite composites

Suppose that electric field solutions of a composite under discussion are generally given by $F_i(x)$, which, in case of a disk ferrite, is replaced by $J_n(x)$, the Bessel function of the order n, where $x = k_e r_j$, $k_e = \omega\sqrt{\varepsilon_0 \varepsilon_e \mu_0 \mu_e}$. Using the electric field solutions, one can obtain the following approximate circulation conditions derived from the relation of corresponding junction mode impedances.

$$Z^{(0)} = j\frac{3}{2}\zeta \frac{F_0(x)}{F_0'(x)} = -jR_c \cot\left(\frac{\varphi}{2}\right), \tag{1}$$

$$Z^{(+)} = j\frac{3}{2}\zeta \frac{F_1(x)}{F_1'(x) - \frac{\kappa}{\mu}F_1(x)} = -jR_c \cot\left(\frac{\varphi}{2} - \frac{\pi}{2}\right),$$

$$Z^{(-)} = j\frac{3}{2}\zeta \frac{F_1(x)}{F_1'(x) + \frac{\kappa}{\mu}F_1(x)} = -jR_c \cot\left(\frac{\varphi}{2} + \frac{\pi}{2}\right).$$

By solving the set of (1), one can obtain, under the condition $\frac{1}{4}(F_1'(x)/F_1(x))\times(F_0(x)/F_0'(x))/(\sin\Psi/\Psi) \ll 1$,

$$R_c/\zeta = \frac{3}{2}\frac{x}{\kappa/\mu}, \tag{2}$$

$$\sin\varphi = \frac{3}{2}\frac{x}{\kappa/\mu}\frac{F_1'(x)}{F_1(x)}, \tag{3}$$

$$4\left(\frac{\kappa/\mu}{x}\right)^2 = -\frac{F_1'(x)\,F_0'(x)}{F_1(x)\,F_0(x)}, \tag{4}$$

where $\zeta = \frac{2\Psi}{\pi}\sqrt{\mu_0\mu_e/\varepsilon_0\varepsilon_e}$, $\mu_e = (\mu^2 - \kappa^2)/\mu$ and $\Psi$ is half an angle subtended by the stripline on the center conductor. By virtue of (4), one can calculate $x - \kappa/\mu$ relationships. The relevant solutions of the two types of composites are shown in the following table.

| Composite and its geometry | Electric field solutions |
|---|---|
| Conductor-ferrite composite 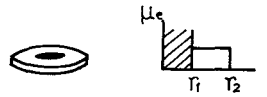 | $J_n(x_2)Y_n(x_1) - Y_n(x_2)J_n(x_1)$, $x_2 = k_e r_2$, $x_1 = k_e r_1$. $x_1/x_2 = r_1/r_2$. |
| Air-ferrite composite 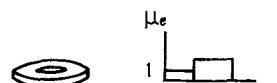 | $J_n(x_3) + C_n Y_n(x_3)$, $C_n = -\frac{J_n'(x_2) - J_n(x_2)D_n}{Y_n'(x_2) - Y_n(x_2)D_n}$, $D_n = \eta_{12}\frac{J_n'(x_1)}{J_n(x_1)}$, $\eta_{12} = \sqrt{\varepsilon_{e1}/\mu_{e2}}\,/\,\varepsilon_{e2}/\mu_{e2}$, $x_3 = k_{e2}r_2$, $x_2 = k_{e2}r_1$, $x_1 = k_{e1}r_1$, |

$x - \kappa/\mu$ relationships of conductor-ferrite composites including a disk are shown in Fig.1. One can understand that the curve of a disk ($r_1/r_2 = 0$) is single-valued with respect to $\kappa/\mu$ and the others are double-valued. As the ratio $r_1/r_2$ increases, a curve moves to a site for large x. Afraid of possible interference from higher modes, one should not choose a geometry of ring for any large $r_1/r_2$. There is, however, the other alternative which is an air-ferrite composite. Fig. 2 refers to the case of air-ferrite composite.

## III. Simplified model of DCFO

As for the resonance modes of a conductor-ferrite composite, the lowest pair of the first order mode is close to those of the disk if the ratio $r_1/r_2$ is small, and the pair moves toward a larger value of x, as $r_1/r_2$ increases. Though the x values of the circulation condition are two-values with respect to $\kappa/\mu$, all circulators of these types are observed to operate only at a single circulation frequency, because only the lowest pair of the first order mode play the central role in circulation. It is also the most fundamental feature which affects the way of designing a circulator.

The circulation condition of an air-ferrite composite appears to be similar to that of a conductor-ferrite composite. The air-ferrite composite is, however, essentially different from a conductor-ferrite composite. The air-ferrite composite has a pair of a certain subsidiary mode just below the ordinary lowest pair. Therefore, two different resonances come to coexist in the range where the ordinary lowest pair is dominant. The subsidiary mode has a degenerate point close to that of the ordinary lowest pair and acts together with the ordinary lowest pair as if the air part has a tensor permeability. Coexistence of the two modes implies to have two operation points under a given external magnetic field.

Suppose now that a composite circulator in question is satisfied with another circulation condition relevant to a junction wave impedance ratio (for convenience, any consideration of impedance adjustment will be excluded here) and the above resonance condition.

Schematic explanation of the circulation will follow in reference to Fig. 3. As the magnetic field changes, the two operation points move in the dynamic operation curves. They are the traces of dynamic operation in a $x - \kappa/\mu$ chart, where the respective resonance curves and the relevant circulation condition are drawn one upon another. As the external magnetic field gradually increases, if a saturation magnetization $4\pi M_s$ is kept constant, the respective resonance points are forced to move almost along the prescribed resonance curves and cross over the curve of the circulation condition at the points A for the subsidiary mode and B for the ordinary mode. These points, A and B, are ideal circulation points that provide two different circulation frequencies $\omega_1$ and $\omega_2$. If A and B are on the same locus of a certain constant magnetic field, they clearly show a perfect DCFO. If they are not, the one that deviates far from the ideal point fails to have a circulation. Then, a feature of DCFO becomes unsymmetric.

An approximate bandwidth for the case of an ideal DCFO is easily estimated to be $(f_2 - f_1) + \delta f$, where $\delta f$ is an average bandwidth of constituent circulations.

## IV. Experiments of DCFO

This schematic explanation was examined by experiments. The ferrite material was of Al-YIG, whose saturation magnetization $4\pi M_s = 950$ Gauss and specific permittivity $\varepsilon_e = 14$. The ring geometry was that $r_2 = 10$ mm, $r_1/r_2 = 0.2$ and the thickness was 2.5 mm. When the external magnetic field was varied in the vicinity of DCFO, the DCFO was observed as shown in Fig. 4. The circulation action had a single peak of isolation (solid lines) in the low frequency site with a small secondary peak in the high frequency site, when the external magnetic field was low. Gradual increasing of the external magnetic field made the secondary peak grow up to a high peak of isolation (dashed lines), after weak DCFO appeared for a while. Then, the peaks of isolation coincided with the bottoms of insertion losses. Those peaks of isolation were translated into the lines (I) for the subsidiary mode and (II) for the normal mode in the $x - \kappa/\mu$ chart which is shown in Fig. 5.

Fig. 6 and 7 show another group of experimental results of DCFO for cases of the following combinations. The same geometry of a stripline Y-junction was applied to all cases. The radius of the ferrite was 10 mm. The ferrite was also Al-YIG, which had two kinds of saturation magnetization: $4\pi M_s = 950$ and 750 Gauss. Three types of the composite for the two kind of saturation magnetization were fabricated. They were $r_1/r_2 = 0.18$, 0.3 and 0.45.

DCFO was observed in the cases of $r_1/r_2 = 0.18$ and 0.3, when the two lowest pairs of the normal and subsidiary modes of the first order joined in circulation. Another example of DCFO was in the case of $r_1/r_2 = 0.45$, when the lowest pair of the normal mode and the lowest (which is not discerned there) and second pairs of the subsidiary mode joined there. Generally speaking, the larger saturation magnetization and separation between the respective pairs, the wider bandwidth. Insertion losses rapidly increased close at the peak of a high frequency site. Since insertion losses are closely related to the secondary circulation adjustment and impedance matching, no conclusion has been made out of the experimental results presented in this paper. One may argue that this rapid increase of insertion losses is caused solely by the characteristics of the same stripline Y-junction. It has been also recognized that the double peaks of isolation can be controlled by changing saturation magnetization and ratio $r_1/r_2$ of a composite.

## V. Conclusions

In order to demonstrate DCFO, a stripline Y-junction circulator was fabricated out of several air-ferrite composites. DCFO is feasible, if both subsidiary mode and normal mode are available. The application of the DCFO has made new types of wideband circulators obtainable. One may also forcast the future of multiple circulation frequency operation. As it is seen in Fig. 5, one more mode is traced above the normal mode. Further theoretical elaboration and more detailed discussions will be reported in near future.

The author wishes to thank Mr. Z. Tanaka for his assistance, and Mr. S. Takata, TDK Co. LTD., for his cooperations.

## References

1. H. Bosma, "On stripline Y-circulation at UHF," IEEE Trans. Microwave Theory Tech., vol. MTT-12, pp. 61-72, Jan. 1964.
2. C. E. Fay and R. L. Comstock, "Operation of the ferrite junction circulator," IEEE Trans. Microwave theory Tech., vol. MTT-13, pp. 15-27, Jan. 1965.
3. J. W. Simon, "Broadband strip-transmission line Y-junction circulators," IEEE Trans. Microwave Theory Tech. vol. MTT-13, pp. 335-345, May, 1965.
4. L. K. Anderson, "An analysis of broadband circulators with external tuning elements," IEEE Trans. Microwave Theory Tech., vol. MTT-15, pp. 42-47, Jan. 1974.
5. E. Schwartz, "Broadband matching of resonant circuits and circulators," IEEE Trans. Microwave Theory Tech., vol. MTT-16, pp. 158-165, Mar. 1968.
6. Y. S. Wu and F. J. Rosenbaum, "Wide-band operation of microstrip circulators," IEEE Trans. Microwave Theory Tech., vol. MTT-22, pp. 849-856, Oct. 1974.
7. H. Bosma, "Junction circulators," in Advances in Microwaves, vol. 6, L. Young, Ed. Academic, New York, 1971.

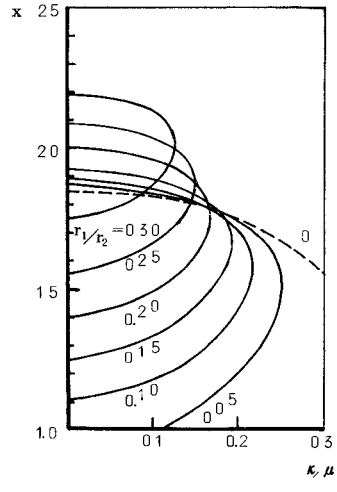


Fig. 1 $x - \kappa/\mu$ relationships for the cases of conductor-ferrite composite (solid lines) and disk (dashed).

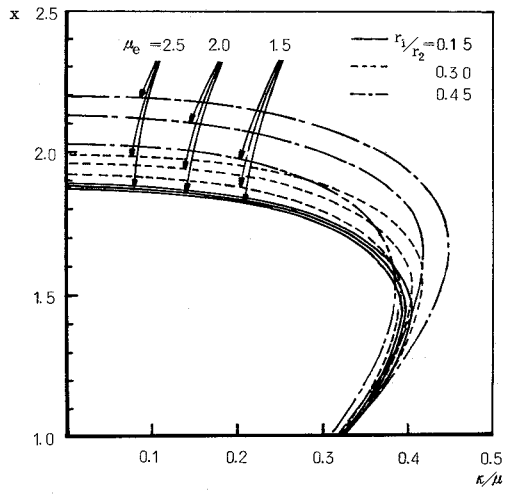


Fig. 2. $x-\kappa/\mu$ relationships for the case of air-ferrite composite.

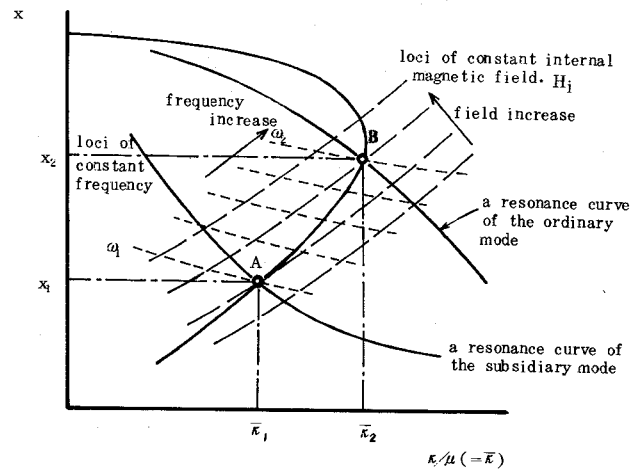


Fig. 3. Schematic illustration of DCFO and plotting of DCFO on the $x-\kappa/\mu$ chart.

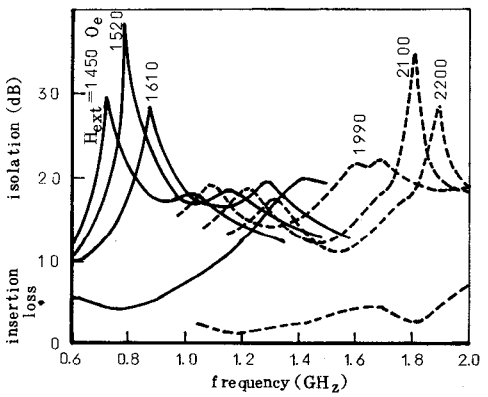


Fig. 4. Examples of isolation characteristics by scanning the external magnetic field $H_{ext}$, for the case of $4\pi M_s$ = 950 Gauss and $r_1/r_2$ = 0.2.

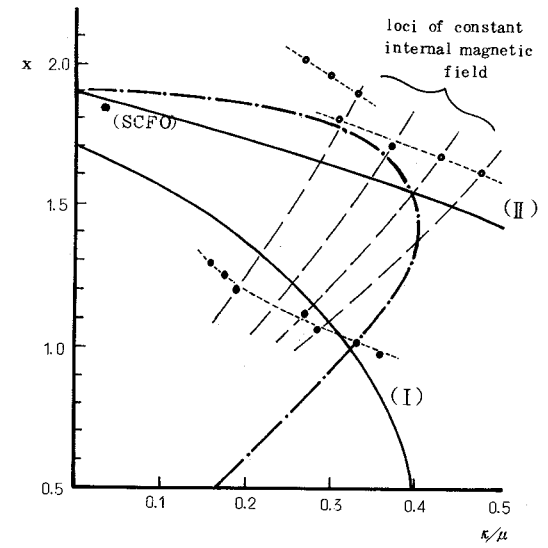


Fig. 5. Translation of isolation peaks shown in Fig. 4 yields dotted curves. Solid lines show resonance curves of the respective constituent modes and dashed lines, loci of constant internal magnetic field $H_i$.

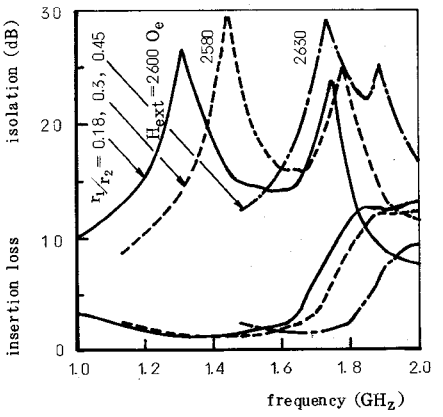


Fig. 6. Experimental examples of DCFO. $4\pi M_s$=950 G. $H_{ext}$=2600, 2580 and 2630 $O_e$. for $r_1/r_2$=0.18, 0.3 and 0.45, respectively.

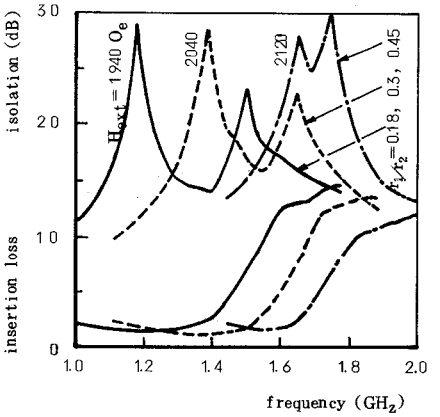


Fig. 7. Experimental examples of DCFO. $4\pi M_s$= 750 G. $H_{ext}$=1940, 2040 and 2120 $O_e$. for $r_1/r_2$= 0.18, 0.3 and 0.45, respectively.